

Surface energy and stress release by layer relaxation

S. K. Kwon,^{1,*} Z. Nabi,¹ K. Kádas,² L. Vitos,^{1,2,3} J. Kollár,² B. Johansson,^{1,3,4} and R. Ahuja^{1,3,†}

¹Condensed Matter Theory Group, Physics Department, Uppsala University, Box 534, SE-751 21 Uppsala, Sweden

²Research Institute for Solid State Physics and Optics, P.O. Box 49, H-1525 Budapest, Hungary

³Applied Materials Physics, Department of Materials Science and Engineering, Royal Institute of Technology, SE-100 44 Stockholm, Sweden

⁴AB Sandvik Materials Technology, SE-811 81 Sandviken, Sweden

(Received 15 September 2005; revised manuscript received 21 October 2005; published 22 December 2005)

The surface energy (γ) and surface stress (τ) for semi-infinite close-packed surfaces of $4d$ transition metals have been calculated using *ab initio* total-energy methods. The moderate agreement between the present and former theoretical data for τ indicates the high level of numerical difficulty associated with such calculations. For the most close-packed surfaces, the present unrelaxed τ values follow the typical trend characteristic for the cohesive energy in nonmagnetic transition-metal series, whereas the relaxed τ values group around ~ 1 mJ/m², obtained for Y, Zr, and Ag, and ~ 3 mJ/m², calculated for Nb, Mo, Tc, Ru, Rh, and Pd. We have found that the average surface energy reduction upon layer relaxation is around 4%. At the same time, a large part of the surface stress is released during the surface relaxation process. To explain the observed behaviors, we have established a simple relationship, which connects the variations of γ and τ to the layer relaxation. This relation reveals the principal factors determining the difference between the surface energy and stress release rates at $4d$ transition-metal surfaces.

DOI: [10.1103/PhysRevB.72.235423](https://doi.org/10.1103/PhysRevB.72.235423)

PACS number(s): 68.47.De, 68.35.Gy, 71.15.Nc, 73.20.-r

Metal surfaces represent the primary window to characterize materials, and form the fundamental interface for many physical and chemical interactions. A properly designed metal surface with controlled chemical compositions may enhance or suppress desirable and undesirable chemical reactions. Furthermore, surfaces with appropriate crystallographic microstructure may improve the tribological properties of metal-metal contacts. Hence gaining atomistic level information on the surface properties has always been one of the central targets of surface physics.

The surface energy (γ) and surface stress (τ) are two basic surface parameters,^{1,2} which are required for modeling a wide variety of surface phenomena, e.g., surface reconstruction, epitaxial growth, and stability of nanoscale particles.^{3,4} In spite of their significant role in surface physics, both the experimental and theoretical values of γ and τ are scarce. Experimental techniques can be used to establish the polar dependence of the surface energy and surface stress,⁵ but a direct measurement of their magnitudes is not yet feasible.^{6,7} During the last decade, theoretical determination of the above surface parameters has gotten within the reach of modern computational physics based on density-functional theory.⁸ Today, it is recognized that carefully performed *ab initio* calculations can yield values of many surface quantities with an accuracy comparable to experiments.^{9–14}

The surface energy is the excess free energy per unit area of a particular crystal facet, and the surface stress gives the atomic-scale in-plane force acting in the surface region. Because the prior is energy and the latter is energy gradient, their numerical calculations require different levels of accuracies in solving the Kohn-Sham density-functional problem. In contrast to the vast number of surface energy calculations, see Refs. 9–13 and references cited therein, only few theoretical investigations on the surface stress are available in the

literature.^{14–19} These independent studies employ different numerical approximations and focus on a specific element or crystal structure. As a consequence, the reported τ values show large scatter, which hinders any attempt to establish general trends of the surface stress across the periodic table. In this work, we present a systematic *ab initio* study of the surface energy and surface stress for the close-packed surfaces of $4d$ transition-metals. We establish a relationship between the variations of γ and τ and the surface layer relaxation, and demonstrate its application to the present database. Our model reveals the principal factors behind the different surface energy and stress release rates at $4d$ transition metal surfaces.

The metal surfaces have been modelled by periodically repeated slabs separated by vacuum layers of thickness equivalent with four to six atomic layers. The slabs were formed by 8 atomic layers for the face centered cubic (fcc) (111) and (100) surfaces, 12 atomic layers for the body centered cubic (bcc) (110) and hexagonal close-packed (hcp) (0001) surfaces, and 16 atomic layers for the bcc (100) surface. The in-plane lattice constant was fixed to the theoretical bulk equilibrium value, and the interlayer distances, except for the central layers, were allowed to relax to their equilibrium values. The surface stress was determined from the variation of the surface energy per atom E^s upon an isotropic in-plane strain $\partial\epsilon$.¹⁴ The slab and the corresponding bulk total energies have been calculated using the projector-augmented wave (PAW) method^{20,21} as implemented in the Vienna Ab-initio Simulation Package.²² The energy cutoff was chosen in the range of 340–460 eV, which assures a bulk total-energy convergence better than 1 meV. For a few selected elements, we have also carried out complementary test calculations within the frameworks of the exact muffin-tin orbitals (EMTO) method.^{23,24} In both *ab initio* methods, the generalized gradient approximation (GGA)(Ref. 25) was em-

TABLE I. Theoretical bulk and surface properties of 4*d* transition metals calculated using the PAW-GGA method. *a* and *c* denote the lattice constants, *B* is the bulk modulus, and $\delta_{1,2,3}$ are the interlayer relaxation rates from the top to down layers. Negative δ corresponds to inward relaxation. The surface energy and surface stress are given for both the unrelaxed (γ_u, τ_u) and relaxed (γ_r, τ_r) surface structures.

		$a(\text{\AA})(c/a)$	<i>B</i> (GPa)	Surface	δ_1 (%)	δ_2 (%)	δ_3 (%)	$\gamma_u(\text{J/m}^2)$	$\gamma_r(\text{J/m}^2)$	$\tau_u(\text{J/m}^2)$	$\tau_r(\text{J/m}^2)$
Y	hcp	3.65(1.55)	41.10	(0001)	-2.37	0.94	0.21	1.01	1.00	1.12	1.00
Zr	hcp	3.23(1.61)	94.12	(0001)	-6.39	2.04	0.25	1.66	1.57	2.22	1.15
Nb	bcc	3.31	170.83	(110)	-4.21	0.60	-0.27	2.10	2.06	4.42	2.99
				(100)	-12.44	-0.50	3.46	2.53	2.32	4.17	0.89
Mo	bcc	3.17	257.32	(110)	-4.74	0.73	0.22	2.81	2.73	4.96	2.96
				(100)	-13.05	4.20	-2.58	3.43	3.15	6.01	1.98
Tc	hcp	2.76(1.60)	295.15	(0001)	-6.70	5.23	-3.03	2.49	2.21	4.75	2.59
Ru	hcp	2.73(1.58)	305.74	(0001)	-3.96	0.12	0.10	2.61	2.52	4.76	3.15
Rh	fcc	3.85	250.61	(111)	-1.80	-0.74	0.63	2.03	2.01	3.41	2.73
				(100)	-4.05	0.42	0.34	2.40	2.35	3.69	2.35
Pd	fcc	3.96	165.59	(111)	0.42	-0.32	-0.07	1.33	1.33	2.58	2.57
				(100)	-1.33	-0.13	0.27	1.52	1.51	2.51	2.16
									2.14 ^c		
Ag	fcc	4.16	89.87	(111)	-0.30	-0.46	0.07	0.76	0.76	0.91	0.79
				(100)	-1.71	0.56	0.25	0.84	0.84	1.47	1.31
									1.75 ^a		
									1.63 ^c		

^aExact muffin-tin orbitals, LDA, Ref. 14.

^bPseudopotential, LDA, Ref. 27.

^cFull potential linear muffin-tin orbitals, LDA, Ref. 16.

^dLinear combination of atomic orbitals, LDA, Ref. 18.

ployed for the exchange-correlation functional. For the reciprocal space integrals, a sufficiently thick *k* mesh was used, so that the total energies were converged to within ~ 0.1 meV/atom.

In Table I, we give a summary of the calculated bulk and surface properties of 4*d* transition metals. The calculated lattice constants and bulk moduli are in excellent agreement with the experimental data.²⁶ The correspondence between the present surface relaxation rates and surface energies and those calculated by the full potential linear muffin-tin orbitals method¹⁰ (not shown) is also satisfactory, especially if one takes into account that in Ref. 10 only the top interlayer distance (δ_1) was relaxed. In Table I, we also list the available theoretical surface stress data obtained in independent *ab initio* calculations.^{14,16,18,27} Except for the Pd (100) surface, our results for both unrelaxed and relaxed τ are smaller compared to the former values. The largest discrepancies are obtained for the (111) surfaces of Pd and Ag. Part of these deviations can be ascribed to the different density functionals employed in different calculations. Note that all the previous theoretical values were obtained within the local-density approximation (LDA) for the exchange-correlation functional. This approximation is known to give about 10–20 % larger surface energies than the GGA used in the present study.¹¹ The deviations between the present and former theoretical τ values arise also from the numerical approximations used in

these calculations. If we let the error connected with such calculations be described by the difference between the LDA results from Table I, and take into account the LDA-GGA difference, the agreement between the present and former theoretical results can be considered satisfactory.

The calculated surface energies and surface stresses for the most close-packed surfaces, viz. fcc (111), bcc (110), and hcp (0001), are plotted in Fig. 1. The surface energies, to a good approximation, follow the Friedel parabola,²⁸ and they are rather insensitive to the surface layer relaxations. The slightly larger surface energy release observed in the case of Tc can be associated with the half filled *d* band. The trend of the unrelaxed surface stress is similar to that of the surface energy. Large stress values ($\tau \sim 2\gamma$) are observed for Nb and Mo (110), Tc (0001), and Ru (0001) surfaces with unrelaxed structures. It is interesting that the surface stress, in contrast to the surface energy, is greatly affected by the surface relaxation. This result is in line with previous observations.⁴ After relaxation, the stresses can be grouped around a large τ (~ 3 J/m²) and a small τ (~ 1 J/m²) value. The surface orientation dependence of τ is also significantly altered by the surface relaxation. For most of the cubic metals, except for Ag, we find that increasing surface roughness lowers the relaxed surface stress. In Ag the most close-packed (111) facet has a lower τ compared to that of the more open (100) facet.

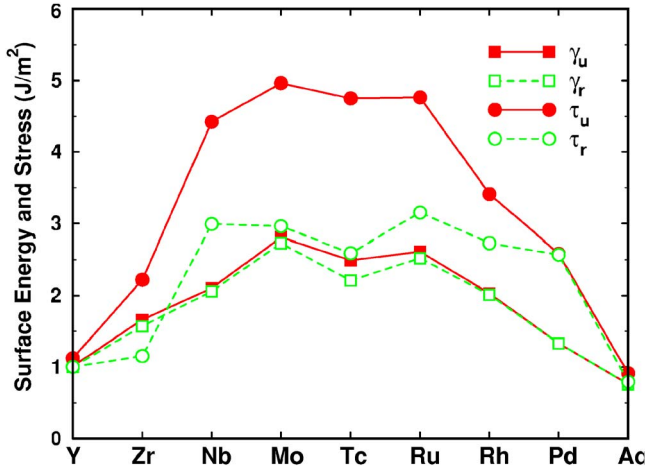


FIG. 1. (Color online) The calculated surface energy (square) and stress (circle) for the most close-packed surfaces of 4d transition metals: hcp (0001) for Y, Zr, Tc, and Ru; bcc (110) for Nb and Mo; and fcc (111) for Rh, Pd, and Ag. Solid and dashed lines connect results obtained for the unreaxed and relaxed surfaces, respectively.

For stable surfaces γ is always a positive quantity, whereas τ can have both positive (compressive) and negative (tensile) values. When a surface is created, the electrons from the out-of-plane dangling bonds are redistributed within the surface layer. This increases the surface in-plane bond energy compared to that in bulk, and thus the minimum of the surface energy per atom $E^s(\varepsilon)$ is located at a negative strain $\bar{\varepsilon}$. Since the surface stress is the slope of $E^s(\varepsilon)$ at $\varepsilon = 0$,¹⁴ the above picture suggests that the surface stress of metals should generally be positive. This is in good agreement with the present findings (Table I). According to the Shuttleworth equation,²⁹ $\tau = \gamma + \partial\gamma/\partial\varepsilon$, the surface energy change upon a surface deformation ($\partial\gamma/\partial\varepsilon$) is negative for $\tau/\gamma < 1$. We find that three 4d metal surfaces meet this condition: the Zr (0001), Nb (100), and Mo (100) surfaces. It is worthwhile to note that these surfaces satisfy the above condition only after the surface relaxation, and their relaxation rates show exceptionally high values (Table I). The τ/γ ratio can be considered as a measure of the in-plane versus out-of-plane surface relaxation rate. Then, surfaces with $\tau/\gamma < 1$ are over-relaxed, and those with $\tau/\gamma > 1$ are under-relaxed. At the same time, the Y (0001), Rh (100), and Ag (111) surfaces are optimally relaxed systems with $\tau/\gamma \sim 1$.

At free surfaces, there is always a tendency to recover part of the lost bonding energy. The surface layer relaxation is one of the main mechanisms in this process. For most of the transition-metal surfaces, the top layer relaxation δ_1 is significantly larger than the relaxations of the subsurface layers $\delta_2, \delta_3, \dots$. Therefore, in the following model, we neglect the relaxations in the subsurface layers, and describe the surface energy and stress changes in terms of the relative top-layer relaxation δ measured from the equilibrium position. The normal component of the surface stress tensor $\tau_{zz} \equiv \partial E^s/A \partial \varepsilon_{zz}$ vanishes at the equilibrium geometry. Hence τ_{zz} can be expanded as $\tau_{zz}(\delta) = C_{\perp} \delta + \mathcal{O}(\delta^2)$, where C_{\perp} is a surface elastic constant. After integrating $\tau_{zz}(\delta)$ between a finite δ and 0, we obtain

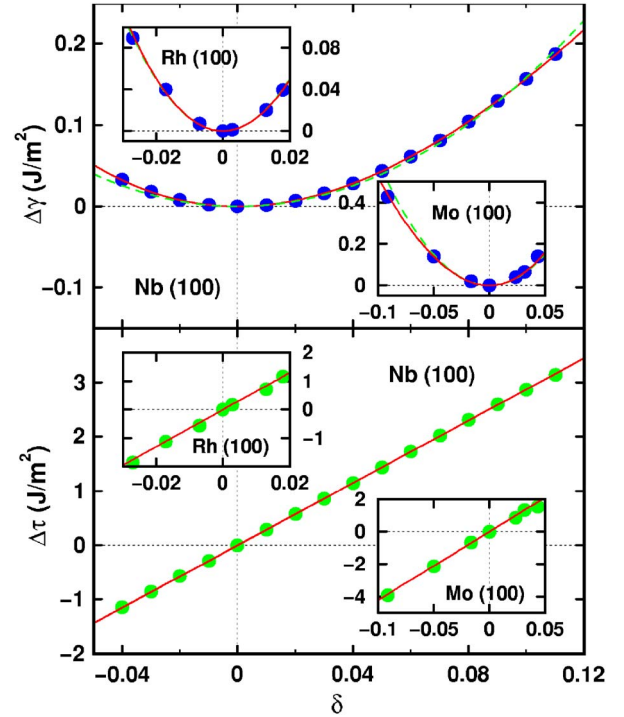


FIG. 2. (Color online) The surface energy ($\Delta\gamma$, upper panel) and stress ($\Delta\tau$, lower panel) changes for the Nb, Mo, and Rh (100) as functions of the top layer relaxation δ . Circles are the calculated values. In the upper panel the solid and dashed lines are cubic and quadratic fitting functions, respectively, and in the lower panel the line is a linear fitting to the calculated points. The results for Nb have been obtained using the PAW method, and those for Rh and Mo (insets) using the EMTO method.

$$\gamma(\delta) = \gamma(0) + \frac{1}{2}C_{\perp}\delta^2 + \mathcal{O}(\delta^3). \quad (1)$$

According to this expression, the variation of the surface energy relative to the fully relaxed equilibrium value $\gamma(0)$, viz. $\Delta\gamma = \gamma(\delta) - \gamma(0)$, can be described approximately as a harmonic function of the top-layer relaxation rate δ . We mention that Eq. (1) expresses the condition that the slab total energy is stationary in δ near the equilibrium layer geometry. To establish the δ dependence of the surface stress, we start from the slab energy density $\epsilon(\varepsilon)$, written as a function of the in-plane strain ε . For a fixed δ , we expand $\epsilon(\varepsilon)$ around the equilibrium surface strain $\bar{\varepsilon}$, viz. $\epsilon(\varepsilon) = \epsilon(\bar{\varepsilon}) + C_{\parallel}(\varepsilon - \bar{\varepsilon})^2/2 + \mathcal{O}[(\varepsilon - \bar{\varepsilon})^3]$, where C_{\parallel} has the meaning of a surface in-plane elastic constant. Taking into account that a similar expansion for the bulk energy density contains no linear term in ε , for $|\bar{\varepsilon}| \ll |\delta|$ we obtain $\tau \approx -C_{\parallel}\bar{\varepsilon}$. Now, expanding this expression around $\delta=0$, we find

$$\tau(\delta) \approx \tau(0) + (C_{\parallel}\bar{\varepsilon})'_0\delta + \mathcal{O}(\delta^2), \quad (2)$$

where the derivative of $C_{\parallel}\bar{\varepsilon}$ is taken at $\delta=0$. In Eq. (2), the linear term appears mainly because of the pronounced δ dependence of $\bar{\varepsilon}$. Our calculations show that for all the considered 4d metal surfaces, the minimum position of $\epsilon(\varepsilon)$, i.e., $\bar{\varepsilon}$,

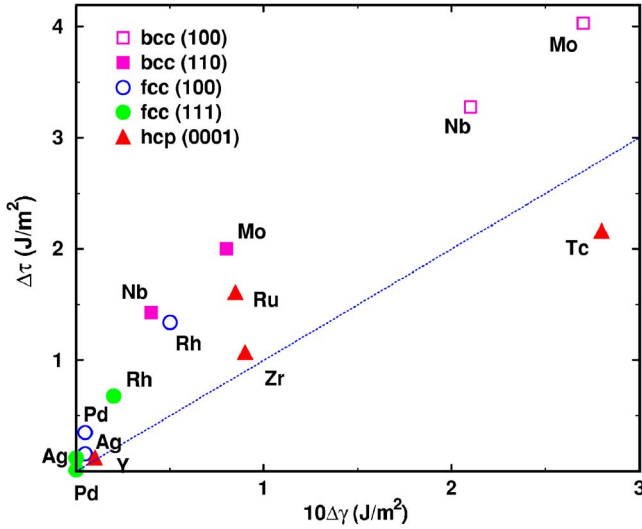


FIG. 3. (Color online) The calculated surface stress change ($\Delta\tau$) versus surface energy ($\Delta\gamma$) change for the $4d$ transition-metal surfaces listed in Table I. The dotted line ($\Delta\tau=10\Delta\gamma$) is to illustrate that for most of the surfaces [except for Tc (0001)] the calculated $\Delta\tau$ is at least one order of magnitude larger than $\Delta\gamma$.

is shifted towards zero with decreasing δ . Therefore the surface stress variation $\Delta\tau=\tau(\delta)-\tau(0)$, unlike the surface energy, contains a first-order term in δ that can change the sign of $\tau(\delta)$ in the strongly over-relaxed regime, i.e., for $\tau/\gamma\ll 1$.

To test the proposed expressions for the surface energy and stress release upon relaxation, we have calculated $\Delta\gamma$ and $\Delta\tau$ as functions of the top layer relaxation rate. Results for the (100) surfaces of Nb, Mo, and Rh are shown in Fig. 2. We chose these surfaces because they exhibit the largest relaxations among the cubic $4d$ metals (Table I). It is quite clear from Fig. 2 that $\Delta\gamma$ and $\Delta\tau$ show qualitatively different behaviors. $\Delta\gamma$ has a minimum at the equilibrium and the calculated points lie close to a second-order polynomial fit (dashed line). At the same time, $\Delta\tau$ is almost a perfectly linearly increasing function of δ . The second-order term in $\Delta\tau$, inherited from $\Delta\gamma$, is totally overshadowed by the dominant linear term from Eq. (2). Figure 2 also demonstrates the validity range of the harmonic approximation for $\gamma(\delta)$. For instance, in the case of Nb, this approximation breaks down for $\delta\lesssim -0.03$, but it holds for large positive δ values up to ~ 0.12 , which corresponds approximately to the unrelaxed Nb (100) surface.

We suggest that the relaxation model, mathematically expressed by Eqs. (1) and (2), is valid for all close-packed $4d$ metal surfaces. In Fig. 3, we have plotted the calculated $\Delta\gamma$ and $\Delta\tau$ values for surfaces from Table I. Different points from the figure correspond to different element and surface orientation, and thus to different δ . We find that all the data points, except that for the Tc (0001) surface, are located near [Pd (111), Ag (111), Ag (100), Zr (0001)] or above the line $\Delta\tau=10\Delta\gamma$. To understand this feature, we introduce the ratio $\Delta\tau/\Delta\gamma$ as a measure of the surface stress change versus surface energy change during the relaxation process. The ratio

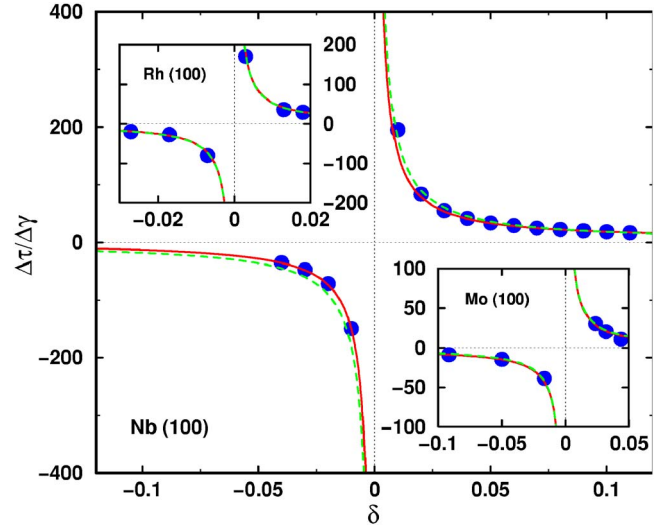


FIG. 4. (Color online) The $\Delta\tau/\Delta\gamma$ ratio for Nb (100), Mo (100) (lower inset), and Rh (100) (upper inset) as a function of δ . Circles are the calculated data (Fig. 2), and dashed lines represent results obtained from Eq. (3). For comparison, values obtained from a cubic fitting to the surface energy (see caption for Fig. 2) are also shown (solid lines). The results for Nb have been obtained using the PAW method, and those for Rh and Mo using the EMTO method.

can be estimated by applying the proposed relaxation dependence of γ and τ . Using the leading terms in Eqs. (1) and (2), we obtain

$$\Delta\tau/\Delta\gamma \approx - \left[\frac{2(C_{\parallel}\bar{\epsilon})'_0}{C_{\perp}} \right] \frac{1}{\delta}. \quad (3)$$

In Fig. 4, we compare the calculated $\Delta\tau/\Delta\gamma$ value for the (100) surfaces of Nb, Mo, and Rh to those obtained from Eq. (3). The good agreement between the two sets of data indicates that the dominant δ -dependent part of $\Delta\tau/\Delta\gamma$ is well captured by Eq. (3). This relation expresses that a large stress release can be present even at surfaces with small layer relaxation, where $\Delta\gamma \rightarrow 0$. As an extreme case, the slightly relaxed (111) surface of Ag ($\delta_1 = -0.30\%$) has $\Delta\gamma \approx 0$ and $\Delta\tau = 0.12 \text{ J/m}^2$. For most of the metal surfaces we have $1/\delta \approx 10\text{--}100$ (Table I). Hence from Eq. (3) we find that $\Delta\tau$ is order of magnitudes larger than $\Delta\gamma$, in perfect accordance with Fig. 3. We note that the scatter of the data points from Fig. 3 reflects the element and surface orientation dependence of the elastic constant anisotropy $[(C_{\parallel}\bar{\epsilon})'_0]/C_{\perp}$ from Eq. (3).

In summary, the surface energy and stress for close-packed surfaces of $4d$ transition-metals have been determined using first-principles methods. The unrelaxed surface stress values for fcc (111), bcc (110), and hcp (0001) surfaces, obtained for ideal surface geometries, follow the typical trend characteristic for the cohesive energy of nonmagnetic transition-metal series. The relaxed surface stress values for the same surfaces, on the other hand, can be grouped into two main groups: Y, Zr, and Ag belong to the low- τ ($\sim 1 \text{ J/m}^2$) group, and the rest of the $4d$ metals to the high- τ ($\sim 3 \text{ J/m}^2$) group. In contrast to the surface energy, a

significant reduction of the surface stress with surface layer relaxation is obtained. This indicates that the surface stability against reconstruction is mainly realized by a giant surface stress release upon layer relaxation and the surface energy change is only of secondary importance in this context. The large stress release versus small surface energy change behavior is explained using a simple relaxation model. We believe that this model will provide a useful information to

analyze different phenomena at metal surfaces.

This work was supported by the Swedish Research Council (VR-SIDA), the Swedish Foundation for Strategic Research, the Swedish Foundation for International Cooperation (STINT), and the Research Project OTKA Grant Nos. T046773 and T048827 of the Hungarian Scientific Research Fund.

*Electronic address: Se.Kyun.Kwon@fysik.uu.se

†Electronic address: Rajeev.Ahuja@fysik.uu.se

¹J. Frenkel and T. Kontorova, Phys. Z. Sowjetunion **13**, 1 (1938).

²M. Mansfield and R. J. Needs, J. Phys.: Condens. Matter **2**, 2361 (1990).

³H. Ibach, Surf. Sci. Rep. **29**, 193 (1997).

⁴P. Müller and A. Saúl, Surf. Sci. Rep. **54**, 157 (2004).

⁵J. J. Métois, A. Saúl, and P. Müller, Nat. Mater. **4**, 238 (2005).

⁶D. Sander, Curr. Opin. Solid State Mater. Sci. **7**, 51 (2003).

⁷A. Mechler, J. Kokavecz, P. Heszler, and R. Lal, Appl. Phys. Lett. **82**, 3740 (2003); P. Heszler, K. Révész, C. T. Reimann, A. Mechler, and Z. Bor, Nanotechnology **11**, 37 (2000).

⁸P. Hohenberg and W. Kohn, Phys. Rev. **136**, B864 (1964); W. Kohn and L. J. Sham, Phys. Rev. **140**, A1133 (1965).

⁹H. L. Skriver, and N. M. Rosengaard, Phys. Rev. B **43**, 9538 (1991).

¹⁰M. Methfessel, D. Hennig, and M. Scheffler, Phys. Rev. B **46**, 4816 (1992).

¹¹L. Vitos, A. V. Ruban, H. L. Skriver, and J. Kollár, Surf. Sci. **411**, 186 (1998).

¹²I. Galanakis, N. Papanikolaou, and P. H. Dederichs, Surf. Sci. **511**, 1 (2002).

¹³H. L. Skriver, A. V. Ruban, J. K. Norskov, L. Vitos, and J. Kollár, Prog. Surf. Sci. **64**, 193 (2000).

¹⁴J. Kollár, L. Vitos, J. M. Osorio-Guillén, and R. Ahuja, Phys. Rev. B **68**, 245417 (2003).

¹⁵R. J. Needs and M. Mansfield, J. Phys.: Condens. Matter **1**, 7555 (1989).

¹⁶V. Fiorentini, M. Methfessel, and M. Scheffler, Phys. Rev. Lett.

71, 1051 (1993).

¹⁷P. J. Feibelman, Phys. Rev. B **50**, 1908 (1994).

¹⁸P. J. Feibelman, Phys. Rev. B **51**, 17867 (1995).

¹⁹P. Gumbsch and M. S. Daw, Phys. Rev. B **44**, 3934 (1991).

²⁰G. Kresse and D. Joubert, Phys. Rev. B **59**, 1758 (1999).

²¹P. E. Blöchl, Phys. Rev. B **50**, 17953 (1994).

²²G. Kresse and J. Hafner, Phys. Rev. B **48**, 13115 (1993); **49**, 14251 (1994).

²³O. K. Andersen, O. Japson, and G. Krier, in *Methods of Electronic Structure Calculations*, edited by V. Kumar, O. K. Andersen, and A. Mookerjee (World Scientific, Singapore, 1994).

²⁴L. Vitos, H. L. Skriver, B. Johansson, and J. Kollár, Comput. Mater. Sci. **18**, 24 (2000); L. Vitos, Phys. Rev. B **64**, 014107 (2001).

²⁵J. P. Perdew and Y. Wang, Phys. Rev. B **45**, 13244 (1992); J. P. Perdew, in *Electronic Structure of Solids '91*, edited by P. Ziesche and H. Eschrig (Akademie Verlag, Berlin, 1991), Vol. 91, p. 11.

²⁶D. A. Young, in *Phase Diagrams of the Elements* (University of California Press, Berkeley, CA, 1991).

²⁷A. Filippetti, V. Fiorentini, K. Stokbro, R. Valente, and S. Baroni, in *Materials Theory of Simulations and parallel algorithms*, edited by E. Kaxiras, J. Joannopoulos, P. Vashishta, and R. K. Kalia, MRS symposia proceedings No. 408 Materials Research Society, Pittsburgh, (1996). P. 457.

²⁸J. Kollár, L. Vitos, B. Johansson, and H. L. Skriver, Phys. Status Solidi B **217**, 405 (2000).

²⁹R. Shuttleworth, Proc. Phys. Soc., London, Sect. A **63**, 445 (1950).